Interactive Multi-Robot Painting Through Colored Motion Trails

María Santos [1,*]**, Gennaro Notomista** [2]**, Siddharth Mayya**[3]**, and Magnus Egerstedt** [1]

[1]*School of Electrical and Computer Engineering, Institute for Robotics and Intelligent Machines, Georgia Institute of Technology, Atlanta, GA, USA*
[2]*School of Mechanical Engineering, Institute for Robotics and Intelligent Machines, Georgia Institute of Technology, Atlanta, GA, USA*
[3]*GRASP Laboratory, University of Pennsylvania, Philadelphia, PA, USA*

Correspondence*:
María Santos
maria.santos@gatech.edu

2 ABSTRACT

In this paper, we present a robotic painting system whereby a team of mobile robots equipped with different color paints create pictorial compositions by leaving trails of color as they move throughout a canvas. We envision this system to be used by an external user who can control the concentration of different colors over the painting by specifying density maps associated with the desired colors over the painting domain, which may vary over time. The robots distribute themselves according to such color densities by means of a heterogeneous distributed coverage control paradigm, whereby only those robots equipped with the appropriate paint will track the corresponding color density function. The painting composition therefore arises as the integration of the motion trajectories of the robots, which lay paint as they move throughout the canvas tracking the color density functions. The proposed interactive painting system is evaluated on a team of mobile robots with different experimental setups in terms of paints given to the robot team to highlight the effects and benefits of considering heterogeneous teams when there is a limited availability of painting resources.

Keywords: interactive robotic art, robotic swarm, painting, human-swarm interaction, heterogeneous multi-robot teams

1 INTRODUCTION

The intersection of robots and arts has become an active object of study as both researchers and artists push the boundaries of the traditional conceptions of different forms of art by making robotic agents dance (Nakazawa et al. (2002); LaViers et al. (2014); Bi et al. (2018)), create music (Hoffman and Weinberg (2010)), support stage performances (Ackerman (2014)), create paintings (Lindemeier et al. (2013); Tresset and Leymarie (2013)), or become art exhibits by themselves (Dean et al. (2008); Jochum and Goldberg (2016); Dunstan et al. (2016); Vlachos et al. (2018)). On a smaller scale, the artistic possibilities of robotic swarms have also been explored in the context of choreographed movements to music (Ackerman (2014); Schoellig et al. (2014); Alonso-Mora et al. (2014)), emotionally expressive motions (**?**Dietz et al. (2017); Levillain et al. (2018); St-Onge et al. (2019)), or interactive music generation based on the interactions between agents (Albin et al. (2012)), among others.

Figure 1. A group of 12 robots generating a painting based on the densities specified by a human user for 5 different color tones: cyan, blue, pink, orange and yellow. The robots lay colored trails as they move throughout the canvas, distributing themselves according to their individual painting capabilities. The painting arises as a result of the motion trails integrating over time.

27   In the context of robotic painting, the focus has been primarily on robotic arms capable of rendering
28   input images according to some aesthetic specifications (Lindemeier et al. (2013); Scalera et al. (2019)), or
29   even reproducing scenes from the robot's surroundings—e.g. portraits (Tresset and Leymarie (2013)) or
30   inanimated objects (Kudoh et al. (2009)). The production of abstract paintings with similar robotic arm
31   setups remains mostly unexplored, with some exceptions (Schubert (2017)). While the idea of swarm
32   painting has been substantially investigated in the context of computer generated paintings, where virtual
33   painting agents move inspired by ant behaviors (Aupetit et al. (2003); Greenfield (2005); Urbano (2005)),
34   the creation of paintings with embodied robotic swarms is lacking. Furthermore, in the existing instances of
35   robotic swarm painting, the generation paradigm is analogous to those employed in simulation: the painting
36   emerges as a result of the agents movement according to some behavioral, preprogrammed controllers
37   (Moura and Ramos (2002); Moura (2016)). The robotic swarm thus acts in a completely autonomous
38   fashion once deployed, which prevents any interactive influence of the human artist once the creation
39   process has begun. Even in such cases where the human artist participates in the creation of the painting
40   along with the multi-robot system (Chung (2018)), the role of the human artist has been limited to that of a
41   co-creator of the work of art, since they can add strokes to the painting but their actions do not influence
42   the operation of the multi-robot team.

43   In this paper, we present a multi-robot painting system based on ground robots that lay color trails as they
44   move throughout a canvas, shown in Fig. 1. The novelty of this approach lies in the fact that an external
45   user—the artist—can influence the movement of robots capable of painting specific colors, thus controlling
46   the concentration of certain pigments on different areas of the painting canvas. Inspired by Diaz-Mercado
47   et al. (2015), this human-swarm interaction is formalized through the use of scalar fields—which we refer
48   to as *density functions*—associated with the different colors such that, the higher the color density specified
49   at a particular point, the more attracted the robots equipped with that color will be to that location. Upon
50   the specification of the color densities, the robots distribute themselves over the canvas in a distributed

51 fashion by executing a controller that optimally covers the density objectives specified by the operator
52 based on the heterogeneous painting capabilities of the robots in the team (Santos et al. (2018); Santos
53 and Egerstedt (2018)). Thus, the system provides the artist with a high-level way to control the painting
54 behavior of the swarm as a whole, agnostic to the total number of robots in the team or the specific painting
55 capabilities of each of them.

56   The remainder of the paper is organized as follows: In Section 2, we formally introduce the problem
57 of coverage control and its extension to heterogeneous robot capabilities as it enables the human-swarm
58 interaction modality used in this paper. Section 3 elaborates on the generation of color densities to be
59 tracked by the multi-robot system along with the color selection strategy adopted by each robot for its
60 colored trail. A series of experiments conducted on a team of differential-drive robots is presented in Section
61 4, where different painting compositions arise as a result of assigning different painting capabilities—both
62 in terms of paints given to the individual robots as well as total paint available—to the multi-robot team.
63 The effects of this heterogeneous resources on the final color distributions observed on the paintings are
64 discussed in Section 5. Section 6 concludes the paper.

2 DENSITY-BASED MULTI-ROBOT CONTROL

65 The interactive multi-robot painting system presented in this paper operates based on the specification
66 of desired concentration of different colors over the painting canvas. As stated in Section 1, this color
67 preeminence is encoded through color density functions that the artist can set over the domain to influence
68 the trajectories of the robots and, thus, produce the desired coloring effect. In this section, we recall the
69 formulation of the coverage control problem as it serves as the mathematical backbone for the human-swarm
70 interaction modality considered in this paper.

2.1 Coverage Control

72   The coverage control problem deals with the question of how to distribute a team of N robots with
73 positions $p_i \in \mathbb{R}^d$, $i \in \{1, \ldots, N\} =: \mathcal{N}$, to optimally cover the environmental features of a domain
74 $D \in \mathbb{R}^d$, $d = 2$ and $d = 3$ for ground and aerial robots, respectively. The question of how well the team is
75 covering a domain is typically asked with respect to a density function, $\phi : D \mapsto [0, \infty)$, that encodes the
76 importance of the points in the domain (Cortes et al. (2004); Bullo et al. (2009)). Denoting the aggregate
77 positions of the robots as $p = [p_1^\mathrm{T}, \ldots, p_N^\mathrm{T}]^\mathrm{T}$, a natural way of distributing coverage responsibilities among
78 the team is to let Robot i be in charge of those points closest to it,

$$V_i(p) = \{q \in D \mid \|q - p_i\| \leq \|q - p_j\|, \ \forall j \in \mathcal{N}\},$$

79 that is, its Voronoi cell with respect to the Euclidean distance. The quality of coverage of Robot i over its
80 region of dominance can be encoded as,

$$h_i(p) = \int_{V_i(p)} \|p_i - q\|^2 \phi(q) \, dq, \tag{1}$$

81 where the square of the Euclidean distance between the position of the robot and the points within its region
82 of dominance reflects the degradation of the sensing performance with distance. The performance of the
83 multi-robot team with respect to ϕ can then be encoded through the locational cost in Cortes et al. (2004),

$$\mathcal{H}(p) = \sum_{i=1}^{N} h_i(p) = \sum_{i=1}^{N} \int_{V_i(p)} \|p_i - q\|^2 \phi(q) \, dq, \tag{2}$$

84 with a lower value of the cost corresponding to a better coverage. A necessary condition for (2) to be
85 minimized is that the position of each robot corresponds to the center of mass of its Voronoi cell (Du et al.
86 (1999)), given by

$$C_i(p) = \frac{\int_{V_i(p)} q\phi(q)\,dq}{\int_{V_i(p)} \phi(q)\,dq}.$$

87 This spatial configuration, referred to as a centroidal Voronoi tessellation, can be achieved by letting the
88 multi-robot team execute the well-known Lloyd's algorithm (Lloyd (1982)), whereby

$$\dot{p}_i = \kappa(C_i(p) - p_i). \tag{3}$$

89 The power of the locational cost in (2) lies on its ability to influence which areas of the domain the robots
90 should concentrate by specifying a single density function, ϕ, irrespectively of the number of robots in the
91 team. This makes coverage control an attractive paradigm for human-swarm interaction, as introduced in
92 Diaz-Mercado et al. (2015), since a human operator can influence the collective behavior of an arbitrarily
93 large swarm by specifying a single density function. In this paper, however, we consider a scenario where a
94 human operator can specify multiple density functions associated with the different colors to be painted
95 and, thus, a controller encoding such color heterogeneity must be considered. The following section recalls
96 a formulation of the coverage problem for multi-robot teams with heterogeneous capabilities and a control
97 law that solves the coverage problem such that all robots move to minimize the locational cost.

98 **2.2 Coverage Control for Teams With Heterogeneous Painting Capabilities**

99   The human-swarm interaction modality considered in this paper allows the artist to specify a set of
100 density functions associated with different colors to produce desired concentrations of colors over the
101 canvas. To this end, we recover the heterogeneous coverage control formulation in Santos and Egerstedt
102 (2018). Let $\mathcal{P}$ be the set of paint colors and $\phi_j : D \mapsto [0, \infty)$, $j \in \mathcal{P}$, the family of densities associated
103 with the colors in $\mathcal{P}$ defined over the convex domain, D, i.e. the painting canvas. In practical applications,
104 the availability of paints given to each individual robot may be limited due to payload limitations, resource
105 depletion, or monetary constraints. To this end, let Robot i, $i \in \mathcal{N}$, be equipped with a subset of the paint
106 colors, $\pi(i) \subset \mathcal{P}$, such that it can paint any of those colors individually or a color that results from their
107 combination. The specifics concerning the color mixing strategy executed by the robots are described in
108 detail in Section 3.

 Analogously to (1), the quality of coverage performed by Robot i with respect to Color j can be encoded
through the locational cost

$$h_i^j(p) = \int_{V_i^j(p)} \|p_i - q\|^2 \phi_j(q)\,dq, \tag{4}$$

where V_i^j is the region of dominance of Robot i with respect to Color j. A natural choice to define the
boundaries of V_i^j is for Robot i to consider those robots in the team capable of painting Color j that are
closest to it. If we denote as $\mathcal{N}^j$ the set of robots equipped with Color j,

$$\mathcal{N}^j = \{i \in \mathcal{N} \mid j \in \pi(i) \subset \mathcal{P}\},$$

(a) Voronoi partition with respect to color blue.   (b) Voronoi partition with respect to color red.
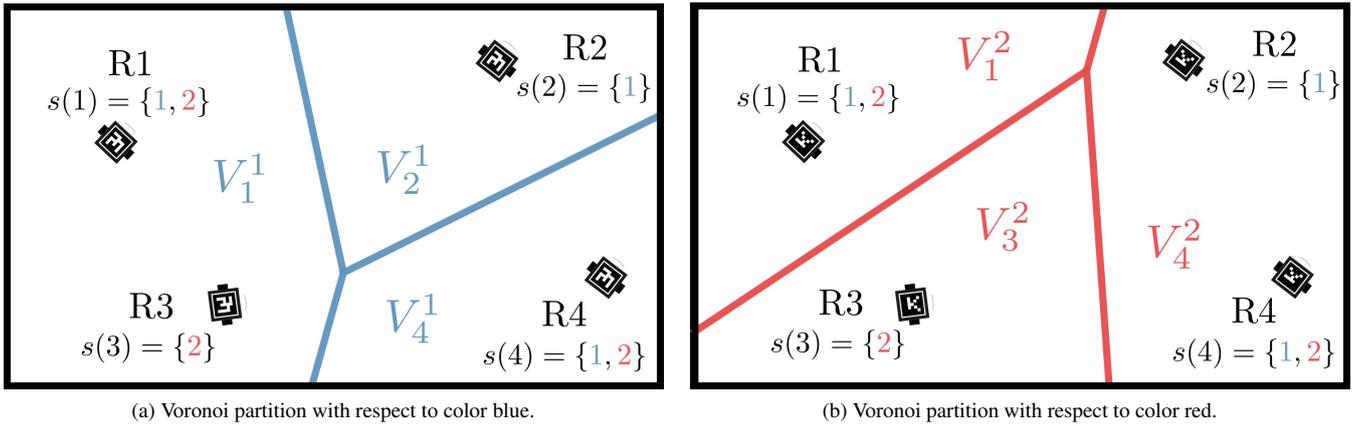
Figure 2. Regions of dominance for four neighboring robots with respect to colors blue (1), (a), and red (2), (b). For each color, the resulting Voronoi cells are generated only by those robots equipped with that painting color. Source: Adapted from Santos and Egerstedt (2018).

then the region of dominance of Robot i with respect to Color $j \in \pi(i)$ is the Voronoi cell in the tessellation whose generators are the robots in $\mathcal{N}^j$,

$$V_i^j(p) = \{q \in D \mid \|p_i - q\| \leq \|p_k - q\|, \forall k \in \mathcal{N}^j\}.$$

Note that, if Robot i is the only robot equipped with Color j, then the robot is in charge of covering the whole canvas, i.e. $V_i^j = D$. Under this partition strategy, as illustrated in Fig. 2, the area that Robot i is responsible for with respect to Color j, V_i^j, can differ from the region to be monitored with respect to Color k, V_i^k, $j, k \in \pi(i)$.

With the regions of dominance defined, we can now evaluate the cost in (4). Thus, the overall performance of the team can be evaluated by considering the complete set of robots and color equipments through the *heterogeneous locational cost* formulated in Santos and Egerstedt (2018),

$$\mathcal{H}_{het}(p) = \sum_{j \in \mathcal{P}} \sum_{i \in \mathcal{N}^j} \int_{V_i^j(p)} \|p_i - q\|^2 \phi_j(q) \, dq, \tag{5}$$

with a lower value of the cost corresponding to a better coverage of the domain with respect to the family of color density functions ϕ_j, $j \in \mathcal{P}$.

Letting Robot i follow a negative gradient descent of $\mathcal{H}_{het}$ establishes the following control law.

THEOREM 1 (Heterogeneous Gradient Descent (Santos and Egerstedt (2018))). *Let Robot i, with planar position p_i, evolve according to the control law $\dot{p}_i = u_i$, where*

$$u_i = \kappa \sum_{j \in \pi(i)} M_i^j(p)(C_i^j(p) - p_i), \tag{6}$$

where $M_i^j(p)$ and $C_i^j(p)$ are, respectively, the heterogeneous mass and center of mass of Robot i with respect to Color j, defined as

$$M_i^j(p) = \int_{V_i^j(p)} \phi_j(q)\, dq, \quad C_i^j(p) = \frac{\int_{V_i^j(p)} q\phi_j(q)\, dq}{M_i^j}. \tag{7}$$

116 *Then, as $t \to \infty$, the robots will converge to a critical point of the heterogeneous location cost in* (5) *under*
117 *a positive gain $\kappa > 0$.*

118 PROOF. See Santos and Egerstedt (2018).

119 Therefore, the controller that minimizes the heterogeneous locational cost in (5) makes each robot
120 move according to a weighted sum where each term corresponds with a continuous-time Lloyd descent—
121 analogous to (3)—over a particular color density ϕ_j, weighted by the mass corresponding to that painting
122 capability.

123 The controller in (6) thus enables an effective human-swarm interaction modality for painting purposes
124 where the artist only has to specify color density functions for the desired color composition and the
125 controller allows the robots in the team to distribute themselves over the canvas according to their
126 heterogeneous painting capabilities. Note that, while other human-swarm interaction paradigms based on
127 coverage control have considered time-varying densities to model the input provided by an external operator
128 (Diaz-Mercado et al. (2015)), in the application considered in this paper heterogeneous formulation of the
129 coverage control problem, while considering static densities, suffices to model the information exchange
130 between the artist and the multi-robot system.

3 FROM COVERAGE CONTROL TO PAINTING

131 In Section 2, we established a human-swarm interaction paradigm that allows the artist to influence the
132 team of robots so that they distribute themselves throughout the canvas according to a desired distribution
133 of color and their painting capabilities. But how is the painting actually created? In this section, we present
134 a strategy that allows each robot to choose the proportion in which the colors available in its equipment
135 should be mixed in order to produce paintings that reflect, to the extent possible, the distributions of color
136 specified by the artist.

137 The multi-robot system considered in this paper is conceived to create a painting by means of each robot
138 leaving a trail of color as it moves over a white canvas. While the paintings presented in Section 4 do
139 not use physical paint but, rather, projected trails over the robot testbed, the objective of this section is to
140 present a color model that both allows the robots to produce a wide range of colors with minimal painting
141 equipment and that closely reflects how the color mixing would occur in a scenario where physical paint
142 were to be employed. To this end, in order to represent a realistic scenario where robots lay physical paint
143 over a canvas, we use the subtractive color mixing model (see Berns (2000) for an extensive discussion in
144 color mixing), which describes how dyes and inks are to be combined over a white background to absorb
145 different wavelengths of white light to create different colors. In this model, the primary colors that act as a
146 basis to generate all the other color combinations are cyan, magenta and yellow (CMY).

147 The advantage of using a simple model like CMY is twofold. Firstly, one can specify the desired presence
148 of an arbitrary color in the canvas by defining in which proportion these should mix at each point and,
149 secondly, the multi-robot system as a collective can generate a wide variety of colors being equipped

150 with just cyan, magenta and yellow paint, i.e. $\mathcal{P} = \{C, M, Y\}$ in the heterogeneous multi-robot control
151 strategy in Section 2.2. The first aspect reduces the interaction complexity between the human and the
152 multi-robot system: the artist can specify a desired set of colors $\mathcal{C}$ throughout the canvas by defining the
153 CMY representation of each color $\beta \in \mathcal{C}$ as $[\beta_C, \beta_M, \beta_Y], \beta_j \in [0, 1], j \in \mathcal{P}$, and its density function
154 over the canvas $\phi_\beta(q), q \in D$. Note that a color specified in the RGB color model (red, green and blue),
155 represented by the triple $[\beta_R, \beta_G, \beta_B]$, can be directly converted to the CMY representation by subtracting
156 the RGB values from 1, i.e. $[\beta_C, \beta_M, \beta_Y] = 1 - [\beta_R, \beta_G, \beta_B]$. Given that the painting capabilities of the
157 multi-robot system are given by $\mathcal{P} = \{C, M, Y\}$, the densities that the robots are to cover according to the
158 heterogeneous coverage formulation in Section 2.2 can be obtained as,

$$\phi_j(q) = \bigoplus_{\beta \in \mathcal{C}} \beta_j \phi_\beta(q), \quad j \in \mathcal{P},$$

159 where $\oplus$ is an appropriately chosen composition operator. The choice of composition operator reflects
160 how the densities associated with the different colors should be combined in order to compute the overall
161 density function associated with each CMY primary color. For example, one way to combine the density
162 functions is to compute the maximum value at each point,

$$\phi_j(q) = \max_{\beta \in \mathcal{C}} \beta_j \phi_\beta(q), \quad j \in \mathcal{P}.$$

163   The question remaining is how a robot should combine its available pigments in its color trail to reflect
164 the desired color density functions. The formulation of the heterogeneous locational cost in (5) implies
165 that Robot i is in charge of covering Color j within the region dominance V_i^j and of covering Color k
166 within V_i^k, $j, k \in \pi(i) \subset \mathcal{P}$. However, depending on the values of the densities ϕ_j and ϕ_k within these
167 Voronoi cells, the ratio between the corresponding coverage responsibilities may be unbalanced. In fact,
168 such responsibilities are reflected naturally through the heterogeneous mass, $M_i^j(p)$, defined in (7). Let us
169 denote as $[\alpha_i^C, \alpha_i^M, \alpha_i^Y], \alpha_i^j \in [0, 1], \alpha_i^C + \alpha_i^M + \alpha_i^Y = 1$, the color proportion in the CMY basis to be
170 used by Robot i in its paint trail. Then, a color mixing strategy that reflects the coverage responsibilities of
171 Robot i can be given by,

$$\alpha_i^j = \frac{M_i^j(p)}{\sum_{k \in \pi(i)} M_i^k(p)}, \quad j \in \pi(i) \subset \mathcal{P}. \tag{8}$$

172 Note that, when $M_i^j(p) = 0, \forall j \in \pi(i) \subset \mathcal{P}$, the robot is not covering any density and, thus, $\alpha_i^j, j \in \mathcal{P}$,
173 can be undefined.

174   Figure 3 illustrates the operation of this painting mechanism for three different density color specifications.
175 Firstly, the mechanism is simulated for a robot equipped with all three colors—cyan (C), magenta (M)
176 and yellow (Y)—in Figs. 3a, 3c and 3e. As seen, the robot lays a cyan trail as it moves to optimally cover
177 a single cyan density function in Fig. 3a. In Fig. 3c, two different density functions are specified, one
178 magenta and one yellow, and the robot lays down a trail whose color is a combination of both paints.
179 Finally, in Fig. 3e, the robot is tasked to cover a density that is a combination of the CMY colors. Since the
180 robot is equipped with all three colors, the trail on the canvas exactly replicates the colors desired by the
181 user.

182   For the same input density specifications, Figs. 3b, 3d, and 3f illustrate the trails generated by a team of 3
183 robots equipped with different subsets of the color capabilities. As seen, the color of the individual robot

(a) Robot: (CMY), Density: ($\beta_1 = (1, 0, 0)$)

(b) Robots: (CMY), (CM), (Y), Density: ($\beta_1 = (1, 0, 0)$)

(c) Robot: (CMY), Densities: $\beta_2 = (0, 1, 0)$, $\beta_3 = (0.0.1)$

(d) Robots: (CMY), (CM), (Y), Densities: $\beta_2 = (0, 1, 0)$, $\beta_3 = (0.0.1)$

(e) Robot: (CMY), Density: $\beta_4 = (0.3, 0.2, 0.2)$

(f) Robots: (CMY), (CM), (Y), Density: $\beta_4 = (0.3, 0.2, 0.2)$
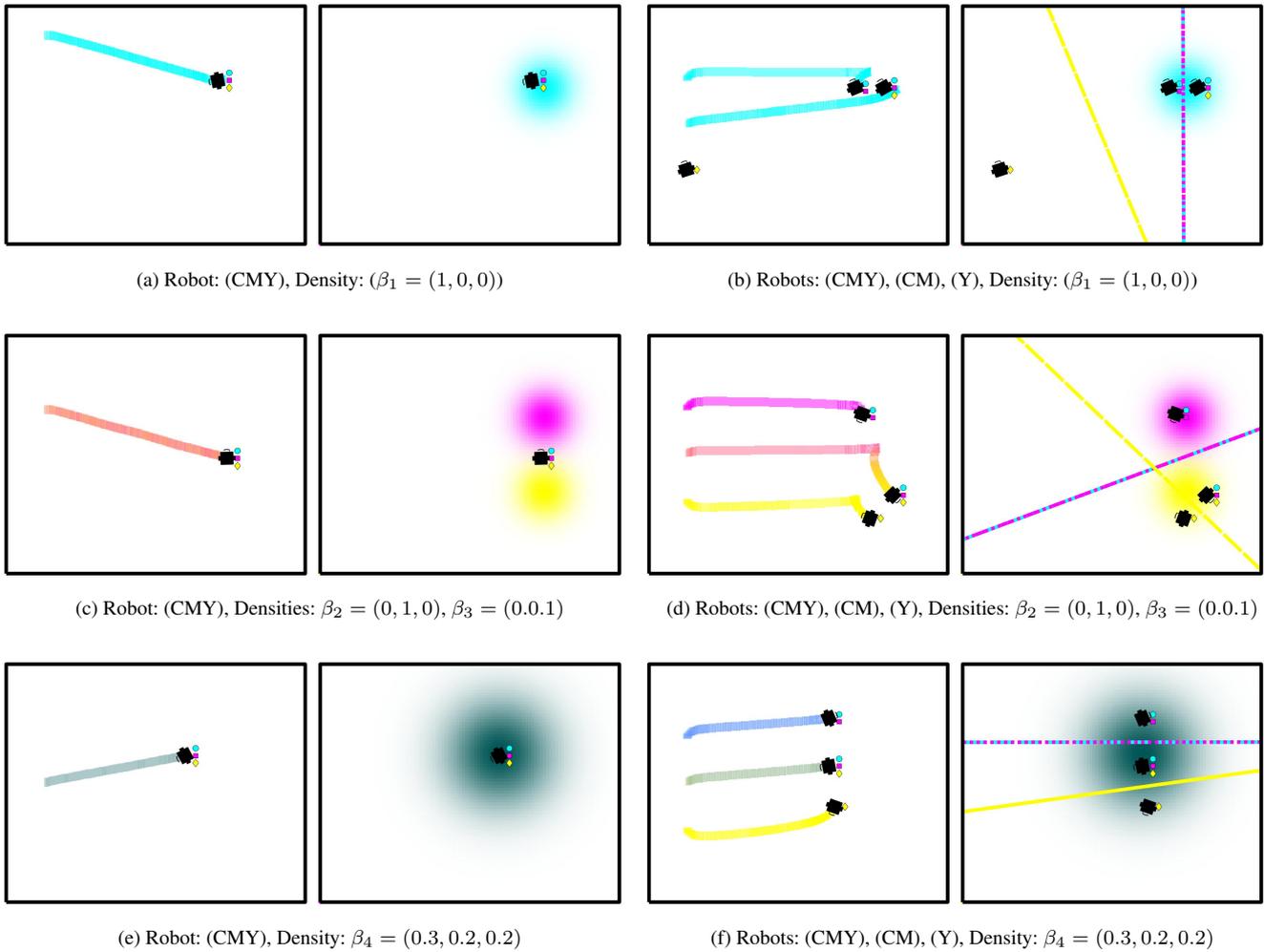
Figure 3. Painting mechanism based on heterogeneous coverage control. Each subfigure shows the color trails laid by the robots (left) as they move to optimally cover a user-specified color density function (right) by executing the controller in (6). The symbols located to the right of the robot indicate its painting capabilities. Figures (a), (c) and (e) show the operation of the painting mechanism in Section 3 for a single robot equipped with all three colors, i.e. cyan (C), magenta (M) and yellow (Y), thus capable of producing all color combinations in the CMY basis. In (a), the robot lays a cyan trail according to the density color specification β_1. The robot equally mixes magenta and yellow in (c) according to the color mixing strategy in (8), producing a color in between the two density color specifications, β_2 and β_3. Finally, in (e), the robot exactly replicates the color specified by β_4. On the other hand, Figures (b), (d) and (f) depict the operation of the painting mechanism with a team of 3 robots, where the Voronoi cells (color coded according to the CMY basis) are shown on the density subfigures.

184 trails evolve as a function of the robot's equipment, the equipments of its neighbors, and the specified input
185 density functions.

4 EXPERIMENTAL RESULTS WITH PROJECTED TRAILS

186 The proposed multi-robot painting system is implemented on the Robotarium, a remotely accessible
187 swarm robotics testbed at the Georgia Institute of Technology (Wilson et al. (2020)). The human-swarm
188 interaction paradigm for color density coverage presented in Section 2 and the trail color mixing strategy
189 from Section 3 are illustrated experimentally on a team of 12 differential drive robots tasked to paint a set of
190 user-defined color density functions over a 2.4×2m canvas. In order to study how the limited availability

Table 1. Experimental parameters associated with the user-specified color density functions.

β	Color	β_C	β_M	β_Y	K	μ_x	μ_y	σ_x	σ_y	A_x	A_y	f_x	f_y
1	Yellow	.0000	.0863	.5569	60	0	0.8	0.22	0.22	1.1	0.1	1/40	0
2	Orange	.0000	.3529	.5569	40	0	0.4	0.22	0.22	1.1	0.1	1/37	2/15
3	Pink	.0549	.5529	.3451	40	0	0	0.22	0.22	1.1	0.1	1/35	0
4	Blue	.4314	.3098	.1373	60	0	-0.4	0.22	0.22	1.1	0.1	1/33	2/15
5	Cyan	.9686	.0353	.0275	40	0	-0.8	0.22	0.22	1.1	0.1	1/30	0
6	Yellow Sun	0	0	1	60	0.5	0.3	0.125	0.125	0.1	0.1	1/5	1/5

191   of painting resources affects the resulting painting, for the same painting task, 9 different experimental
192   setups in terms of paint equipment assigned to the multi-robot team are considered. While no physical
193   paint is used in the experiments included in this paper, the effectiveness of the proposed painting system is
194   illustrated by visualizing the robots' motion trails over the canvas with an overhead projector.

195   The experiment considers a scenario where the multi-robot team has to simultaneously cover a total of
196   six different color density functions over a time horizon of 300 seconds. The color density functions are of
197   the form,

$$\phi_\beta(q) = \frac{K}{2\pi\sigma_x\sigma_y} \exp\left(-\frac{(q_x - \bar{\mu}_x)^2 + (q_y - \bar{\mu}_y)^2}{2\sigma_x^2\sigma_y^2}\right), \tag{9}$$

with $\beta \in \{1, \ldots, 6\} = \mathcal{C}$, $q = [q_x, q_y]^\mathrm{T} \in D$. The color associated with each density as well as its
parameters are specified in Table 1, and $\bar{\mu}_x$ and $\bar{\mu}_y$ are given by

$$\bar{\mu}_x = \mu_x - A_x \sin(2 * \pi f_x t),$$
$$\bar{\mu}_y = \mu_y - A_y \sin(2 * \pi f_y t).$$

198   Figure 4 illustrates the evolution of the painting for a specific equipment setup as the robots move to cover
199   these densities at $t = 100$s and $t = 300$s.

200   In order to evaluate how the heterogeneous painting capabilities of the multi-robot team affect the
201   outcome of the painting process, the coverage of the color densities is evaluated for 9 different equipment
202   configurations. Table 2 outlines the color painting capabilities available to each of the robots in the different
203   experimental setups. The paintings which result from five of these configurations (the ones with an odd
204   setup ID) are shown in Fig. 5. For the purpose of benchmarking, a simulated painting is generated for
205   painting setup 1, i.e. with complete painting capabilities, under the same heterogeneous density coverage
206   control and color mixing strategies as in the robotic experiments (Fig. 5a). Given the paintings in Figs.
207   5b to 5f, we can observe how the closest color distribution to the simulated painting is achieved in Fig.
208   5b, which corresponds to the case where all the robots have all the painting capabilities—i.e. the team is
209   homogeneous—and, thus, can reproduce any combination of colors in the CMY basis.

210   It is interesting to note the significant changes in the characteristics of the painting for different equipment
211   configurations of the robots. For equipment setups 3, 5, 7 and 9, where some robots—or all—are not
212   equipped with all the color paints, the corresponding paintings do not show as smooth color gradients as
213   the one in Fig. 5b. However, the distribution of color for these paint setups still qualitatively reflects the
214   color specification given by the densities in Table 1. Even in the extreme case of Equipment 9 (see Fig.

(a) $t = 100$s

(b) $t = 300$s
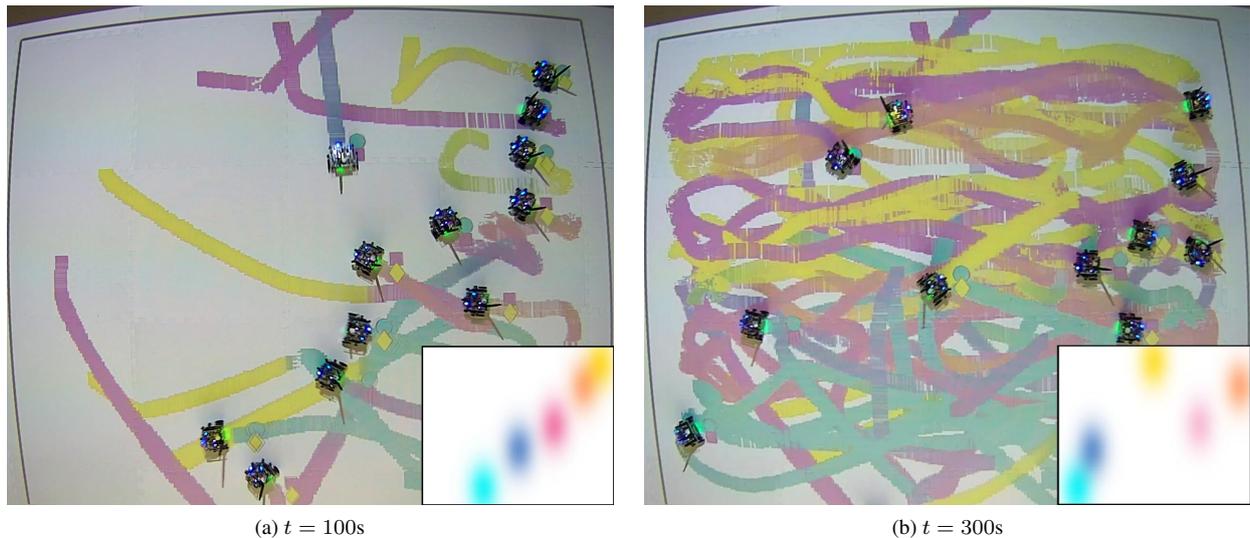
Figure 4. Evolution of the painting according to the density parameters in Table 1, for the Setup 3 given as in Table 2. The robots distribute themselves over the domain in order to track the density functions as they evolve through the canvas. The color distribution of the color trails reflects the colors specified for the density functions within the painting capabilities of the robots. Even though none of the robots is equipped with the complete CMY equipment and, thus, cannot reproduce exactly the colors specified by the user, the integration of the colors over time produce a result that is close to the user's density specification.

215 5f), where none of the robots is equipped with all CMY paints—in fact, half of the robots only have one
216 paint and the other half have pairwise combinations—the robot team still renders a painting that, while
217 presenting colors with less smooth blending than the other setups, still represents the color distribution
218 specified by the densities in Table 1. For setups 3 and 7, the team has the same total number of CMY
219 painting capabilities but the distribution is different among the team members: in Setup 3 none of the robots
220 are equipped with the three colors, while in Setup 7 there are some individuals that can paint any CMY
221 combination and others can paint only one color. Observing the Figs. 5c and 5e, while the resulting colors
222 are less vibrant for the equipment in Setup 3, there seems to be a smoother blending between them along
223 with the vertical axis. Setup 7 produces a painting where overall the colors are more faithful to the ideal
224 outcome presented in Fig. 5a, but that also contain stronger trails corresponding to the pure primary colors
225 appear throughout the painting. If we compare Figs. 5e and 5d we can see how, by adding a small amount
226 of painting capabilities to the system, the color gradients are progressively smoothed. This observation
227 suggests to further analyze the variations that appear on the paintings as a function of the heterogeneous
228 equipment configurations of the different setups. This will be the focus of the next section.

5 DISCUSSION

229 As described in Section 1, the robotic painting system developed in this paper generates illustrations via
230 an interaction between the color density functions specified by the user and the different color equipment
231 present on the robots. In particular, the different equipments not only affect the color trails left by the robots,
232 but also affect their motion as they track the density functions corresponding to their equipment. While
233 Fig. 5 qualitatively demonstrates how the nature of the painting varies with different equipment setups,
234 this section presents a quantitative analysis of the variations among paintings resulting from different
235 equipment setups. We also analyze the reproducibility characteristics of the multi-robot painting system,
236 by investigating how paintings vary among different realizations using the same equipment setups.

Table 2. Paint equipment for the different experimental setups.

Setup ID	ID	Paint Equipment															Total	Heterogeneity	
		1	2	3	4	5	6	7	8	9	10	11	12	13	14	15		Sunset	8-bit RGB
1	C	×	×	×	×	×	×	×	×	×	×	×	×				12		
	M	×	×	×	×	×	×	×	×	×	×	×	×				12	0	0
	Y	×	×	×	×	×	×	×	×	×	×	×	×				12		
2	C	×			×		×	×	×	×	×	×	×	×	×	×	12		
	M		×		×	×		×	×	×	×	×	×	×	×	×	12	.2786	.2680
	Y			×		×	×	×	×	×	×	×	×	×	×	×	12		
3	C	×	×			×	×	×	×			×	×				8		
	M	×	×	×	×			×	×	×	×						8	.3060	.2963
	Y			×	×	×	×			×	×	×	×				8		
4	C	×		×	×	×		×		×	×	×	×				9		
	M		×	×		×	×	×	×		×	×	×				9	.3340	.3121
	C		×	×		×	×		×	×	×	×	×				9		
5	C	×			×		×	×	×	×	×	×	×				9		
	M		×		×	×		×	×	×	×	×	×				9	.3921	.3783
	Y			×		×	×	×	×	×	×	×	×				9		
6	C	×	×				×	×	×	×	×	×					8		
	M			×	×		×	×	×	×	×	×					8	.4488	.4398
	Y					×	×	×	×	×	×	×	×				8		
7	C	×			×	×		×	×	×	×	×					8		
	M		×		×	×	×	×		×	×	×					8	.5686	.5498
	Y			×			×	×	×	×	×	×	×				8		
8	C	×	×	×						×	×	×					6		
	M				×	×	×			×	×	×					6	.6904	.6835
	Y							×	×	×	×	×	×				6		
9	C	×	×				×	×			×	×					6		
	M			×	×		×	×	×	×							6	.8148	.8004
	Y					×	×		×	×	×	×					6		

237 Let S denote the number of distinct equipment setups of the robots in the team—where each unique
238 configuration denotes a robot *species*. We denote $s_\iota \in [0, 1]$ as the probability that a randomly chosen agent
239 belongs to species ι, $\iota \in \mathcal{S} = \{1, \ldots, S\}$, such that

$$\sum_{\iota=1}^{S} s_\iota = 1, \quad \text{and } s = [s_1, \ldots, s_S]^{\mathrm{T}}.$$

240 For each equipment setup in Table 2, these probabilities can be calculated as a function of how many agents
241 are equipped with each subset of the paint colors.

242 We adopt the characterization developed in Twu et al. (2014), and quantify the heterogeneity of a
243 multi-robot team as,

$$H(s) = E(s)Q(s), \tag{10}$$

(a) Simulated painting, Setup 1	(b) Setup 1	(c) Setup 3
(d) Setup 5	(e) Setup 7	(f) Setup 9
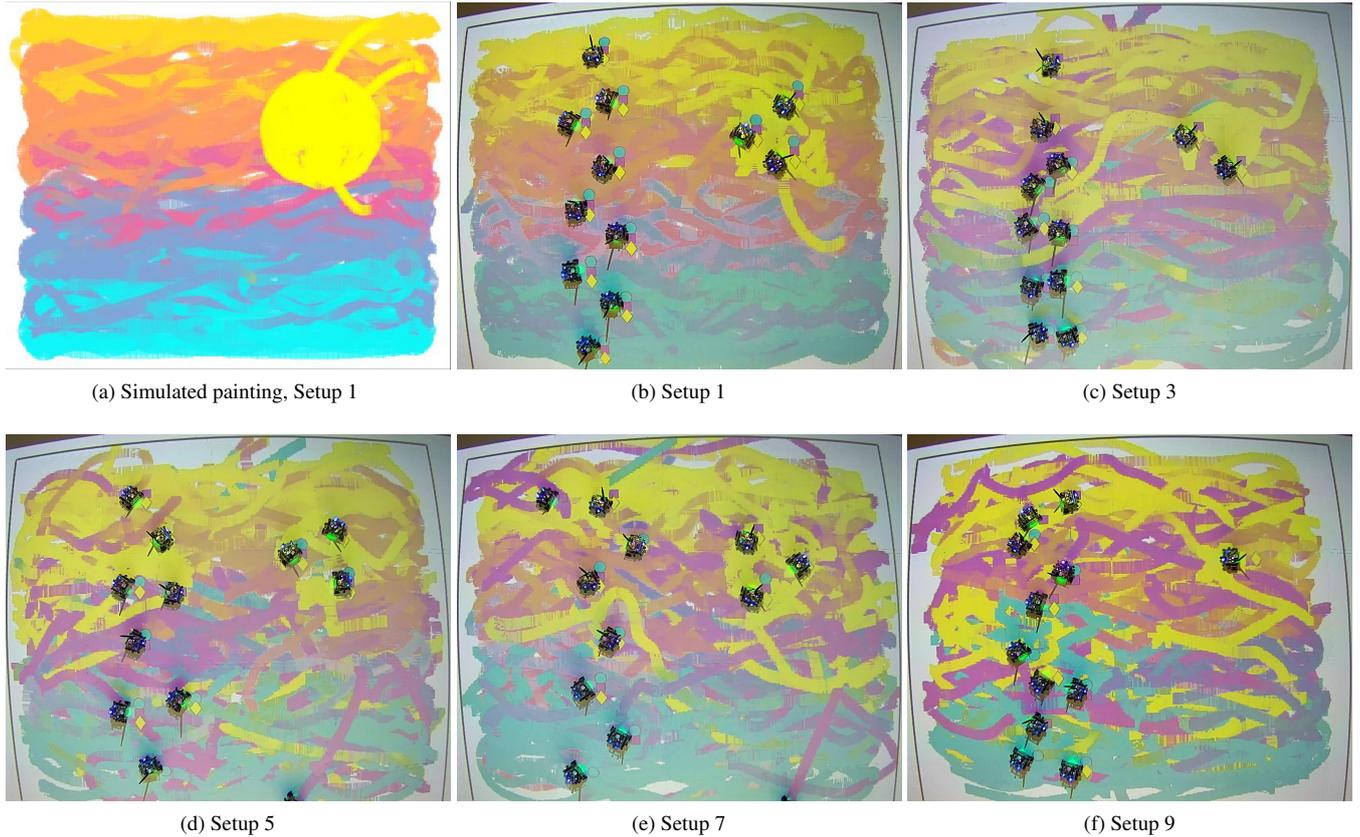
Figure 5. Paintings generated for the densities in (9), with the team of 12 robots in their final positions. Figure 5a corresponds to a simulated painting and it is used for benchmarking. According to the painting equipment setups in Table 2 we can see how, as the robots in the team are equipped with more painting capabilities, the color gradients become smoother and more similar to the ideal outcome.

244   where $E(s)$ represents the *complexity* and $Q(s)$, the *disparity* within the multi-robot system for a given
245   experimental setup, s. More specifically, $E(s)$ can be modeled as the *entropy* of the multi-agent system,

$$E(s) = -\sum_{\iota=1}^{S} s_\iota \log(s_\iota),$$

246   and $Q(s)$ is the *Rao's Quadratic Entropy*,

$$Q(s) = \sum_{\iota=1}^{S}\sum_{\kappa=1}^{S} s_\iota s_\kappa \delta(\iota,\kappa)^2, \tag{11}$$

247   with $\delta : \mathcal{S} \times \mathcal{S} \mapsto \mathbb{R}_+$ a metric distance between species of robots. More specifically, δ represents the
248   differences between the abilities of various species *in the context of performing a particular task*. For
249   example, if we have three robots, one belonging to species s_5 ($\pi(s_5) = \{C\}$) and two belonging to species
250   s_8 ($\pi(s_8) = \{C, M, Y\}$) and we have to paint only cyan, then the distance between agents should be zero,
251   since all of them can perform the same task. However, if the task were to paint a combination of yellow
252   and magenta, then the species s_5 could not contribute to that task and, therefore, $\delta > 0$.

Similar to Twu et al. (2014), we formalize this idea by introducing a task space, represented by the tuple (T, γ) where T denotes the set of tasks, and $\gamma : T \mapsto \mathbb{R}_+$ represents an associated weight function. In this paper, the set of tasks T simply correspond to the different colors specified by the user, as shown in Table 1. Consequently, a task $t_\beta^j \in T$ corresponds to the component j, $j \in \{C, M, Y\}$, of color input $\beta \in \mathcal{C}$. The corresponding weight functions for the tasks are calculated as,

$$\gamma(t_\beta^j) = \frac{\beta_j}{\displaystyle\sum_{\tilde{\beta} \in \mathcal{C}} \sum_{k \in \mathcal{P}} \tilde{\beta}_k}.$$

With this task-space, the task-map, $\omega : \mathcal{S} \mapsto 2^T$, as defined in Twu et al. (2014), directly relates the different robot species with the CMY colors, i.e., if the color equipment of species ι is denoted as $\pi(\iota)$, then it can execute tasks t_β^j if $j \in \pi(\iota)$.

Having defined the task-space, (T, γ), and the task-map, ω, the distance between two agents i and j can be calculated as in Twu et al. (2014),

$$\delta(T, \gamma, \omega)(\iota, \kappa) = \frac{\displaystyle\sum_{t \in (\omega(\iota) \cup \omega(\kappa)) \backslash (\omega(\iota) \cap \omega(\kappa))} \gamma(t)}{\displaystyle\sum_{u \in (\omega(\iota) \cup \omega(\kappa))} \gamma(u)}.$$

This task-dependent distance metric between different robot species can then be used to compute the *disparity* as shown in (11).

Having completely characterized the disparity, $Q(s)$, and the complexity, $E(s)$, of an experimental setup under a specific painting task, one can compute the heterogeneity measure associated with them according to (10). To this end, the third column in Table 2 represents the heterogeneity measure of the different setups. The heterogeneity values have been computed for the sunset-painting task from Table 1, as well as for a generic painting task that considers the whole 8-bit RGB color spectrum as objective colors to be painted by the team. This latter task is introduced in this analysis with the purpose of serving as a baseline to evaluate the comprehensiveness of the proposed sunset painting task. As it can be observed in Table 2, the heterogeneity values obtained for the sunset and the 8-bit RGB tasks are quite similar and the relative ordering of the setups with respect to the heterogeneity measure is the same, thus suggesting that the sunset task used in this paper requires a diverse enough set of painting objectives for all the equipment setups proposed. Armed with this quantification of team heterogeneity, we now analyze how the spatial characteristics of the painting differ as the equipment configurations change.

5.1 Color Distance

We first analyze the complex interplay between motion trails and equipment setups by computing the spatial distance between the mean location of the desired input density function specified by the user, and the resulting manifestation of the color in the painting. To this end, we use the *color distance* metric introduced in Androutsos et al. (1998) to characterize the distance from the color obtained in every pixel of the resulting painting to each of the input colors specified in Table 1.

(a) Simulated painting, Setup 1   (b) Setup 1   (c) Setup 3

(d) Setup 5   (e) Setup 7   (f) Setup 9
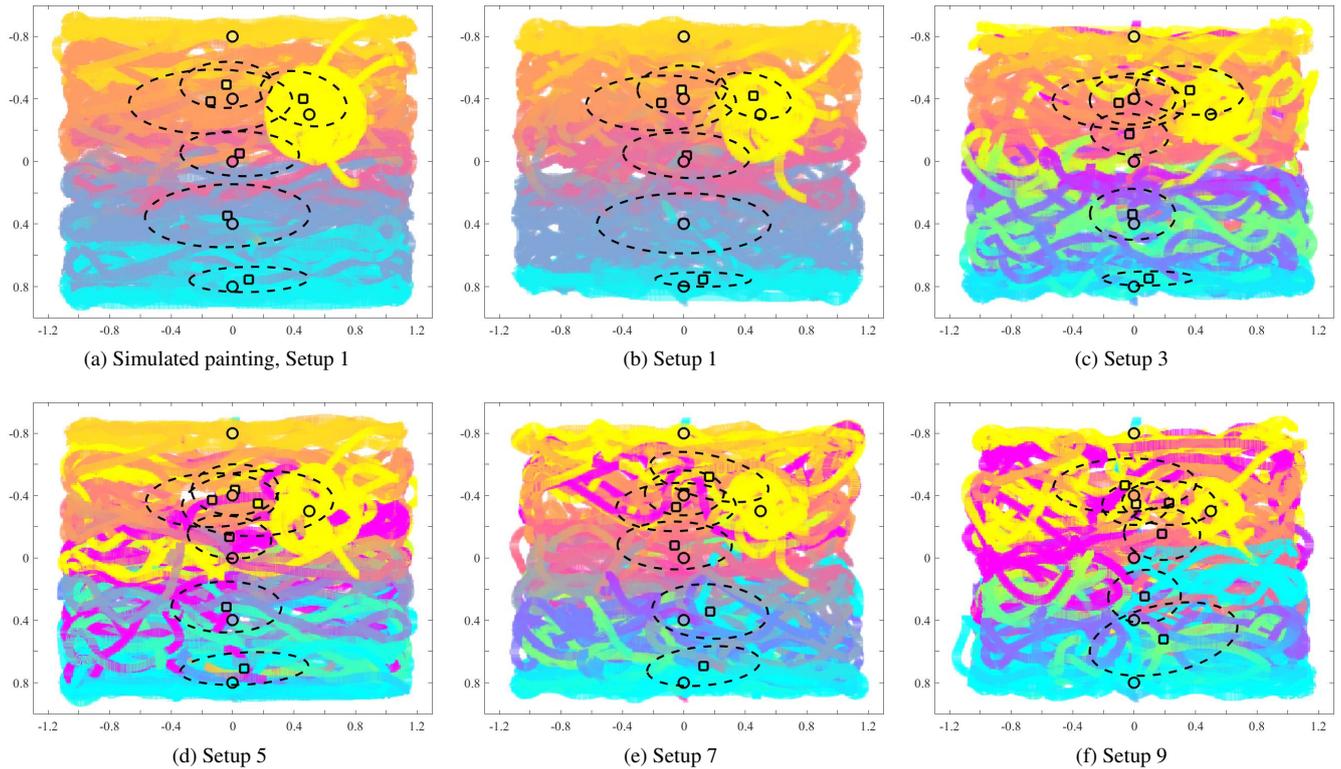
Figure 6. For each input color (given in Table 1): mean of the input density function (circle), and center of mass of the resulting color according to (13). The dotted lines depict the covariance ellipse according to (14). As seen the heterogeneity of the multi-robot team (as defined in (10)) impacts how far the colors are painted from the location of the input, as given by the user.

Let $\rho(q)$ represent the 8-bit RGB vector value for a given pixel q in the painting. Then, the color distance between two pixels q_i and q_j is given as,

$$d_p(q_i, q_j) = 1 - \left[1 - \frac{2}{\pi} \cos^{-1} \left(\frac{\rho(q_i) \cdot \rho(q_j)}{\|\rho(q_i)\|\|\rho(q_j)\|} \right) \right] \left[1 - \frac{\|\rho(q_i) - \rho(q_j)\|}{\sqrt{3 \cdot 255^2}} \right] \qquad (12)$$

Using (12), we can compute the distance from the color of each pixel to each of the input colors specified by the user (given in this paper by Table 1). For a given pixel in the painting q and input color β, these distances can be interpreted as a color-distance density function over the domain, denoted as φ

$$\varphi(q, \beta) = \exp \left(-\frac{d_p(q, \beta)}{\varsigma^2} \right),$$

where, with an abuse of notation, $d_p(q, \beta)$ represents the color distance between the color β and the color at pixel q. For the experiments conducted in this paper, ς^2 was chosen to be 0.1.

Since we are interested in understanding the spatial characteristics of colors in the painting, we compute the center of mass of a particular color β in the painting,

$$C_\beta = \frac{\int_D q\varphi(q, \beta)\, dq}{\int_D \varphi(q, \beta)\, dq}. \qquad (13)$$
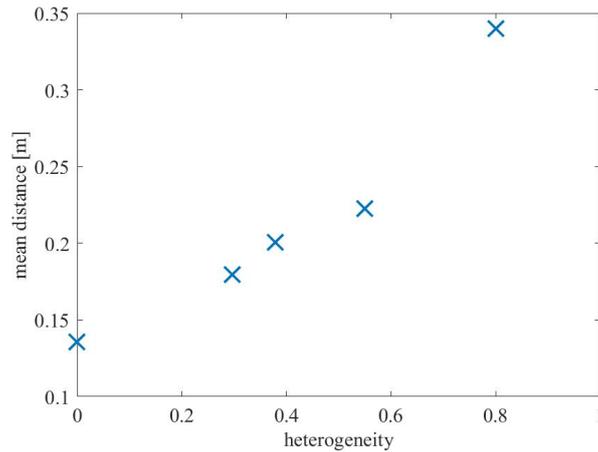
Figure 7. Average distance from mean density input to the resulting center of mass over the input colors of the painting as a function of the heterogeneity among the robots (as defined in (10)). As seen, with increasing sparsity of painting equipment on the robots (signified by increasing heterogeneity), the mean distance increases, indicating that colors get manifested farther away from where the user specifies them.

292 The covariance ellipse for the color β at a pixel q is given as,

$$V_\beta(q) = \sqrt{(\varphi(q))}(q - C_\beta). \tag{14}$$

293 For each of the input colors, Fig. 6 illustrates the extent to which the color center of masses (computed
294 by (13) and depicted by the square filled by the corresponding color) are different from the mean locations
295 of the input density functions (depicted by the circle). For all the painting equipment setups in Fig. 6, as the
296 heterogeneity of the team increases, the mean of the input density function for each color and the resulting
297 center of mass become progressively more distant. This phenomenon is illustrated in Fig. 7, where the
298 mean distance between the input density and the resulting color center of mass is plotted as a function of
299 the heterogeneity of the equipment of the robots. For a given painting P, this distance is computed as,

$$d_c(P) = \frac{\sum_{\beta \in \mathcal{C}} \|\mu_\beta - C_\beta\|}{|\mathcal{C}|}, \tag{15}$$

300 where $\mathcal{C}$ represents the set of input colors, and μ_β represents the mean of the input density function for color
301 β. As seen, with increasing heterogeneity, the mean distance increases because lesser painting capabilities
302 on the robots do not allow them to exactly reproduce the input color distributions. However, even with
303 highly heterogeneous setups, such as Setups 7 or 9, the multi-robot team is still able to preserve highly
304 distinguishable color distributions throughout the canvas, which suggests that the coverage control paradigm
305 for multi-robot painting is quite robust to highly heterogeneous robot teams and resource deprivation.

306 **5.2 Chromospectroscopy**

307 The second method we utilize to quantify the differences among the paintings as a function of the
308 heterogeneity in the robot team is using *chromospectroscopy* (Kim et al. (2014)), which analyzes the
309 frequency of occurrence of a particular color over the canvas. To this end, the painting is divided according
310 to the sectors described in Table 3, which are closely related to the areas of high incidence of the objective
311 color densities in Table 1. A histogram representing the frequency of occurrence of each input color per
312 sector is described in Fig. 8. For the purposes of the chromospectroscopy analysis, the 8-bit RGB color
313 map of the canvas is converted into a 5-bit RGB color map, by reducing the resolution of the color map

Table 3. Color sectors throughout the painting used for the chromospectroscopy analysis, according to the density parameters specified in Table 1.

Sector ID	Objective Color	x_{min}[m]	x_{max}[m]	y_{min}[m]	y_{max}[m]
1	Yellow	-1.2	1.2	1	0.6
2	Orange	-1.2	1.2	0.6	0.2
3	Pink	-1.2	1.2	0.2	0.2
4	Blue	-1.2	1.2	-0.2	-0.6
5	Cyan	-1.2	1.2	-0.6	-1
6	Yellow Sun	0.3	0.7	0.5	0.1

(a) Simulated painting, Setup 1   (b) Setup 1   (c) Setup 3

(d) Setup 5   (e) Setup 7   (f) Setup 9
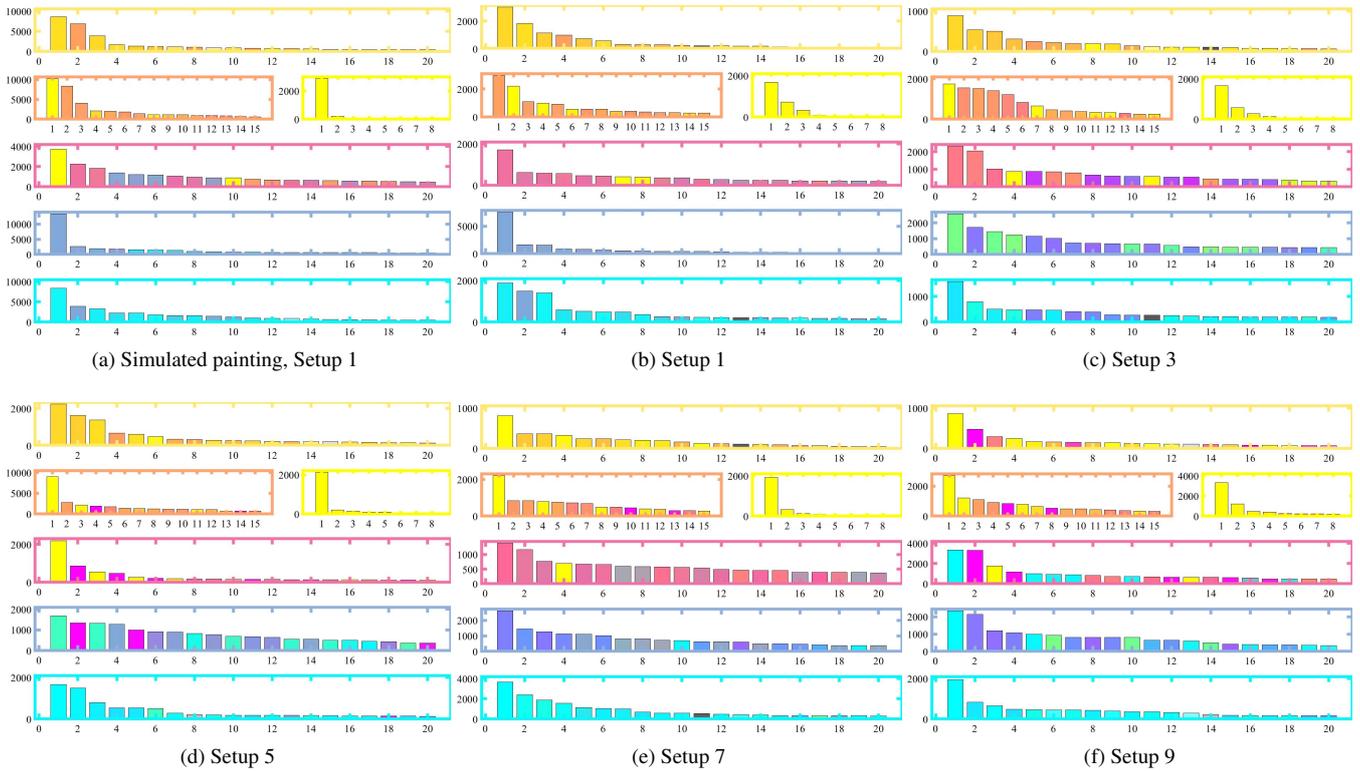
Figure 8. Chromospectroscopy by sectors on the canvas (as indicated in Table 3) for each equipment configuration (as specified in Table 2). With increasing heterogeneity, and consequently, sparser painting capabilities of the robots, colors distinctly different from the target colors begin to appear in each sector. For teams with lower heterogeneity (Setups 1-3), anomalous colors in the chromospectroscopy typically appear from neighboring sectors only.

and grouping very similar colors together, i.e., for an input color $\beta \in [0, 255]^3$, the modified color for the chromospectroscopy analysis in Fig. 8 is computed as $\bar{\beta} = \frac{\beta}{b}$, with $b = 2^3$.

As seen in Fig. 8, the heterogeneity of the robot team significantly affects the resulting color distribution within each sector. More specifically, as the heterogeneity of the team increases, thus depriving the team of painting capabilities, the canvas presents more outlier colors which are present outside the corresponding target sectors. This is apparent in highly heterogeneous teams (Setup 9), where magenta-like colors appear in the top-most sector and cyan appears in the central sector. The three central sectors show a high occurrence of non-target colors. For slightly lesser heterogeneous teams, while the occurring colors often

322 do not correspond with the target colors in the sectors—e.g. green in Sector 4 of Setup 3—, the colors
323 seem consistent in their presence and correspond to limitations on the equipment of the robots: in Setup
324 3, all robots are equipped with only two colors, thus no robot is able to exactly replicate any target color
325 with 3 CMY components by itself. In the case of teams with low heterogeneity, e.g., Setup 1 and Setup 3,
326 resulting colors are mostly consistent with the input target colors. The presence of some colors which do
327 not match the input corresponds to colors belonging to the neighboring sectors. Some specific examples
328 of this include: (i) Setup 1: the presence of yellow in Sector 3, orange in Sector 2, and Blue in Sector 5,
329 (ii) Setup 3: the presence of orange in Sector 1, and blue in Sector 5, (iii) Setup 5: magenta and cyan-like
330 colors in Sector 4.

331   Indeed, as one could expect, the chromospectroscopy reveals that color distributions become less precise
332 as the differences in the painting capabilities of the robots become more acute—observable as distinct
333 paint streaks in Fig. 5 which stand out from the surrounding colors. Nevertheless, the distribution of colors
334 on each sector still matches the color density inputs even for the case of highly heterogeneous teams,
335 which suggests that the multi-robot painting paradigm presented in this paper is robust to limited painting
336 capabilities on the multi-robot team due to restrictions on the available paints, payload limitations on the
337 robotic platforms, or even the inherent resource depletion that may arise from the painting activity.

338 ## 5.3 Statistical Results

339   In order to understand if the statistics reported above remain consistent for multiple paintings generated
340 by the robotic painting system, we ran 10 different experiments for each of the 9 equipment configurations
341 described in Table 2. Figure 9 shows the average of the paintings generated for each equipment, along
342 with the color density averages, computed using (13). Although averaging the 10 rounds seems to dampen
343 the presence of outliers, we can still observe how the distance between the objective color (represented
344 by a circle) and the resulting color distribution (square) generally increases as the team becomes more
345 heterogeneous. Furthermore, if we observe the color gradient along the vertical axis of the painting, the
346 blending of the colors becomes more uneven as the heterogeneity of the team increases. This phenomenon
347 becomes quite apparent if we compare the top row of Fig. 9—(a) to (c)—to the bottom row—(g) to (i).

348   Quantitatively, this distancing between objective and obtained color density distribution is summarized in
349 Fig. 10, which shows the mean distance between the input density and the resulting colors. Analogously to
350 the analysis in Fig. 7, which contained data for one run in the Robotarium for five out of the nine setups,
351 the average distances shown in Fig. 10 show that the resulting color distributions tend to deviate from the
352 objective ones as the team becomes more heterogeneous.

353   The results observed in this statistical analysis, thus, support the observations carried out in the analysis
354 of the paintings obtained in the Robotarium. Therefore, the characterization of the painting outcome with
355 respect to the resources of the team seems consistent throughout different runs and independent of the
356 initial spatial conditions of the team.

6 CONCLUSIONS

357 This paper presents a robotic swarm painting system based on mobile robots leaving trails of paint as
358 they move where a human user can influence the outcome of the painting by specifying desired color
359 densities over the canvas. The interaction between the human artist and the painting is enabled by means of
360 a heterogeneous coverage paradigm where the robots distribute themselves over the domain according to
361 the desired color outcomes and their painting capabilities, which may be limited. A color mixing strategy
362 is proposed to allow each robot to adapt the color of its trail according to the color objectives specified
363 by the user, within the painting capabilities of each robot. The proposed multi-robot painting system
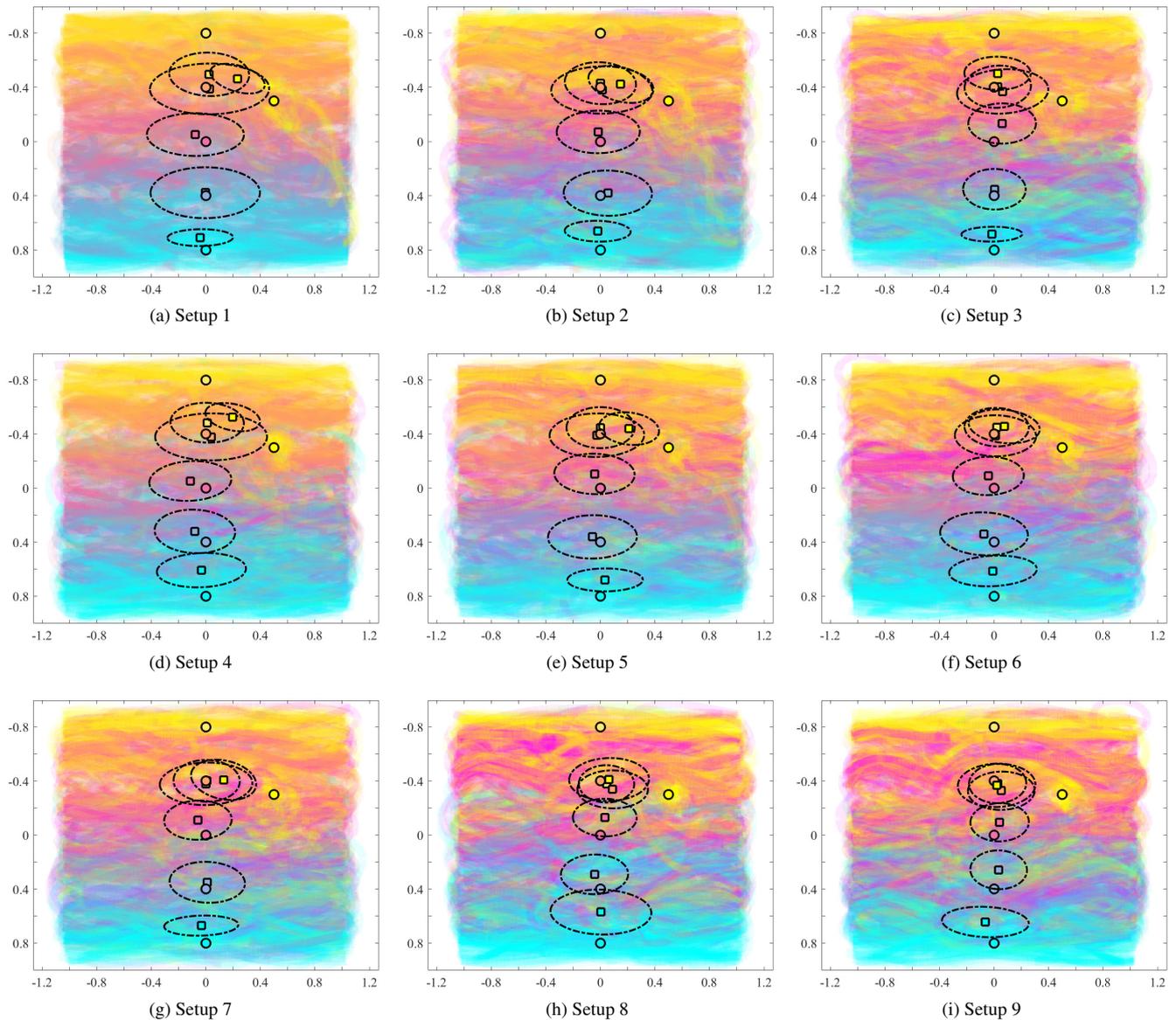
Figure 9. Averaged paintings over 10 trials. Mean of the input densities (circle), center of mass of the resulting colors according to φ from (13) (square), and covariance ellipse (dotted lines). The heterogeneity in the painting equipment of the robots has a significant impact on the nature of the paintings.

is evaluated experimentally to assess how the proposed color mixing strategy and the color equipments of the robots affect the resulting painted canvas. A series of experiments are run for a set of objective density functions, where the painting capabilities of the team are varied with the objective of studying how varying the painting equipment among the robots in the team affects the painting outcome. Analysis of the resulting paintings suggests that, while higher heterogeneity results in bigger deviations with respect to the user-specified density functions—as compared to homogeneous, i.e. fully equipped, teams—the paintings produced by the control strategy in this paper still achieve a distribution of color over the canvas that closely resembles the input even when the team has limited resources.
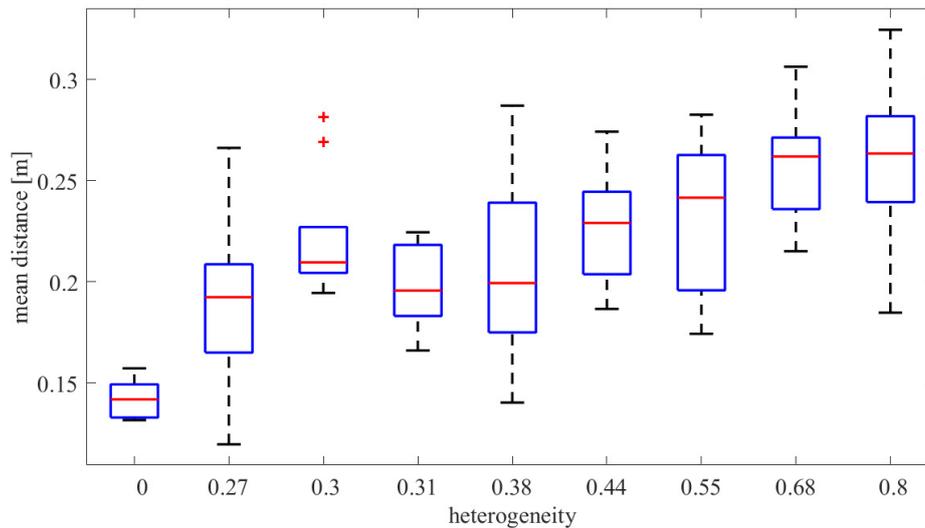
Figure 10. Box plots of the average distance between mean density input to resulting center of mass as computed in (15) for the 9 different equipment configurations. The results are presented for 10 different experiments conducted for each equipment. As seen, the average distance increases with increasing heterogeneity among the robots' painting equipment.

CONFLICT OF INTEREST STATEMENT

372 The authors declare that the research was conducted in the absence of any commercial or financial
373 relationships that could be construed as a potential conflict of interest.

AUTHOR CONTRIBUTIONS

374 All authors listed have made a substantial and intellectual contribution to the work, and approved it for
375 publication.

FUNDING

REFERENCES

378 Ackerman, E. (2014). Flying LampshadeBots Come Alive in Cirque du Soleil. *IEEE Spectrum*
379 Albin, A., Weinberg, G., and Egerstedt, M. (2012). Musical abstractions in distributed multi-robot systems.
380   In *2012 IEEE/RSJ International Conference on Intelligent Robots and Systems*. 451–458
381 Alonso-Mora, J., Siegwart, R., and Beardsley, P. (2014). Human-Robot swarm interaction for entertainment:
382   From animation display to gesture based control. In *Proceedings of the 2014 ACM/IEEE International
383   Conference on Human-robot Interaction* (New York, NY, USA: ACM), HRI '14, 98–98
384 Androutsos, D., Plataniotiss, K. N., and Venetsanopoulos, A. N. (1998). Distance measures for color
385   image retrieval. In *Proceedings 1998 International Conference on Image Processing. ICIP98 (Cat.
386   No.98CB36269)*. vol. 2, 770–774 vol.2
387 Aupetit, S., Bordeau, V., Monmarche, N., Slimane, M., and Venturini, G. (2003). Interactive evolution of
388   ant paintings. In *The 2003 Congress on Evolutionary Computation, 2003. CEC '03*. vol. 2, 1376–1383
389   Vol.2
390 Berns, R. (2000). *Billmeyer and Saltzman's Principles of Color Technology* (New York: Wiley), 3 edn.

391 Bi, T., Fankhauser, P., Bellicoso, D., and Hutter, M. (2018). Real-time dance generation to music for a
392   legged robot. In *2018 IEEE/RSJ International Conference on Intelligent Robots and Systems (IROS)*
393   (Madrid), 1038–1044

394 Bullo, F., Cortes, J., and Martinez, S. (2009). *Distributed Control of Robotic Networks: A Mathematical*
395   *Approach to Motion Coordination Algorithms*. Applied Mathematics Series (Princeton, NJ, USA:
396   Princeton University Press)

397 Chung, S. (2018). Omnia per omnia. `https://sougwen.com/project/omniaperomnia`,
398   Accessed 2019-09-08

399 Cortes, J., Martinez, S., Karatas, T., and Bullo, F. (2004). Coverage control for mobile sensing networks.
400   *IEEE Transactions on Robotics and Automation* 20, 243–255

401 Dean, M., D'Andrea, R., and Donovan, M. (2008). *Robotic Chair* (Vancouver, B.C.: Contemporary Art
402   Gallery)

403 Diaz-Mercado, Y., Lee, S. G., and Egerstedt, M. (2015). Distributed Dynamic Density Coverage for
404   Human-Swarm Interactions. In *American Control Conference (ACC), 2015*. 353–358. doi:10.1109/ACC.
405   2015.7170761

406 Dietz, G., E, J. L., Washington, P., Kim, L. H., and Follmer, S. (2017). Human perception of swarm
407   robot motion. In *Proceedings of the 2017 CHI Conference Extended Abstracts on Human Factors in*
408   *Computing Systems* (Denver, Colorado), 2520–2527

409 Du, Q., Faber, V., and Gunzburger, M. (1999). Centroidal voronoi tessellations: Applications and algorithms.
410   *SIAM Review* 41, 637–676. doi:10.1137/S0036144599352836

411 Dunstan, B. J., Silvera-Tawil, D., Koh, J. T. K. V., and Velonaki, M. (2016). Cultural robotics: Robots as
412   participants and creators of culture. In *Cultural Robotics*, eds. J. T. Koh, B. J. Dunstan, D. Silvera-Tawil,
413   and M. Velonaki (Cham: Springer International Publishing), 3–13

414 Greenfield, G. (2005). Evolutionary methods for ant colony paintings. In *Applications of Evolutionary*
415   *Computing*, eds. F. Rothlauf, J. Branke, S. Cagnoni, D. W. Corne, R. Drechsler, Y. Jin, P. Machado,
416   E. Marchiori, J. Romero, G. D. Smith, and G. Squillero (Berlin, Heidelberg: Springer Berlin Heidelberg),
417   478–487

418 Hoffman, G. and Weinberg, G. (2010). Gesture-based human-robot jazz improvisation. In *2010 IEEE*
419   *International Conference on Robotics and Automation*. 582–587

420 Jochum, E. and Goldberg, K. (2016). *Cultivating the Uncanny: The Telegarden and Other Oddities*
421   (Singapore: Springer Singapore). 149–175

422 Kim, D., Son, S.-W., and Jeong, H. (2014). Large-scale quantitative analysis of painting arts. *Scientific*
423   *Reports* 4, 7370

424 Kudoh, S., Ogawara, K., Ruchanurucks, M., and Ikeuchi, K. (2009). Painting robot with multi-fingered
425   hands and stereo vision. *Robotics and Autonomous Systems* 57, 279 – 288

426 LaViers, A., Teague, L., and Egerstedt, M. (2014). *Style-Based Robotic Motion in Contemporary Dance*
427   *Performance* (Cham: Springer International Publishing). 205–229

428 Levillain, F., St-Onge, D., Zibetti, E., and Beltrame, G. (2018). More than the sum of its parts: Assessing
429   the coherence and expressivity of a robotic swarm. In *2018 IEEE International Symposium on Robot*
430   *and Human Interactive Communication (RO-MAN)*. 583–588. doi:10.1109/ROMAN.2018.8525640

431 Lindemeier, T., Pirk, S., and Deussen, O. (2013). Image stylization with a painting machine using semantic
432   hints. *Computers & Graphics* 37, 293 – 301

433 Lloyd, S. (1982). Least squares quantization in PCM. *IEEE Transactions on Information Theory* 28,
434   129–137. doi:10.1109/TIT.1982.1056489

435 Moura, L. (2016). *Machines That Make Art*. 255–269. doi:10.1007/978-981-10-0321-9_13

Moura, L. and Ramos, V. (2002). *Swarm Paintings—Nonhuman Art* (Lyon/Villeurbanne, France: Architopia: Book, Art, Architecture, and Science, Institut d'Art Contemporain)

Nakazawa, A., Nakaoka, S., Ikeuchi, K., and Yokoi, K. (2002). Imitating human dance motions through motion structure analysis. In *IEEE/RSJ International Conference on Intelligent Robots and Systems*. vol. 3, 2539–2544

Santos, M., Diaz-Mercado, Y., and Egerstedt, M. (2018). Coverage control for multirobot teams with heterogeneous sensing capabilities. *IEEE Robotics and Automation Letters* 3, 919–925

Santos, M. and Egerstedt, M. (2018). Coverage control for multi-robot teams with heterogeneous sensing capabilities using limited communications. In *2018 IEEE/RSJ International Conference on Intelligent Robots and Systems (IROS)* (Madrid, Spain), 5313–5319

Scalera, L., Seriani, S., Gasparetto, A., and Gallina, P. (2019). Watercolour robotic painting: a novel automatic system for artistic rendering. *Journal of Intelligent & Robotic Systems* 95, 871–886

Schoellig, A. P., Siegel, H., Augugliaro, F., and D'Andrea, R. (2014). *So You Think You Can Dance? Rhythmic Flight Performances with Quadrocopters* (Cham: Springer International Publishing). 73–105

Schubert, A. (2017). *An optimal control based analysis of human action painting motions*. Ph.D. thesis, Heidelberg, Germany

St-Onge, D., Levillain, F., Elisabetta, Z., and Beltrame, G. (2019). Collective expression: how robotic swarms convey information with group motion. *Paladyn, Journal of Behavioral Robotics* 10, 418–435. doi:10.1515/pjbr-2019-0033

Tresset, P. and Leymarie, F. F. (2013). Portrait drawing by paul the robot. *Computers & Graphics* 37, 348 – 363

Twu, P., Mostofi, Y., and Egerstedt, M. (2014). A measure of heterogeneity in multi-agent systems. In *2014 American Control Conference*. 3972–3977

Urbano, P. (2005). Playing in the pheromone playground: Experiences in swarm painting. In *Applications of Evolutionary Computing*, eds. F. Rothlauf, J. Branke, S. Cagnoni, D. W. Corne, R. Drechsler, Y. Jin, P. Machado, E. Marchiori, J. Romero, G. D. Smith, and G. Squillero (Berlin, Heidelberg: Springer Berlin Heidelberg), 527–532

Vlachos, E., Jochum, E., and Demers, L. (2018). Heat: The harmony exoskeleton self - assessment test. In *2018 27th IEEE International Symposium on Robot and Human Interactive Communication (RO-MAN)*. 577–582. doi:10.1109/ROMAN.2018.8525775

Wilson, S., Glotfelter, P., Wang, L., Mayya, S., Notomista, G., Mote, M., et al. (2020). The robotarium: Globally impactful opportunities, challenges, and lessons learned in remote-access, distributed control of multirobot systems. *IEEE Control Systems Magazine* 40, 26–44